Electronic Supplementary Material for:

Reflective and transparent cellulose-based passive radiative coolers

Sampath Gamage[1,2], Debashree Banerjee[1,2,§], Md. Mehebub Alam[1,§], Tomas Hallberg[3], Christina Åkerlind[3], Ayesha Sultana[1,2], Ravi Shanker[1,2], Magnus Berggren[1,2], Xavier Crispin[1,2], Hans Kariis[3], Dan Zhao[1], and Magnus P. Jonsson[1,2,*]

[1]Laboratory of Organic Electronics, Department of Science and Technology, Linköping University, SE-601 74 Norrköping, Sweden

[2]Wallenberg Wood Science Center, Linköping University, SE-601 74 Norrköping, Sweden

[3]FOI-Swedish Defense Research Agency, Department of Electro-Optical systems, 581 11 Linköping, Sweden

[§]These authors contributed equally to this work

*Email: magnus.jonsson@liu.se

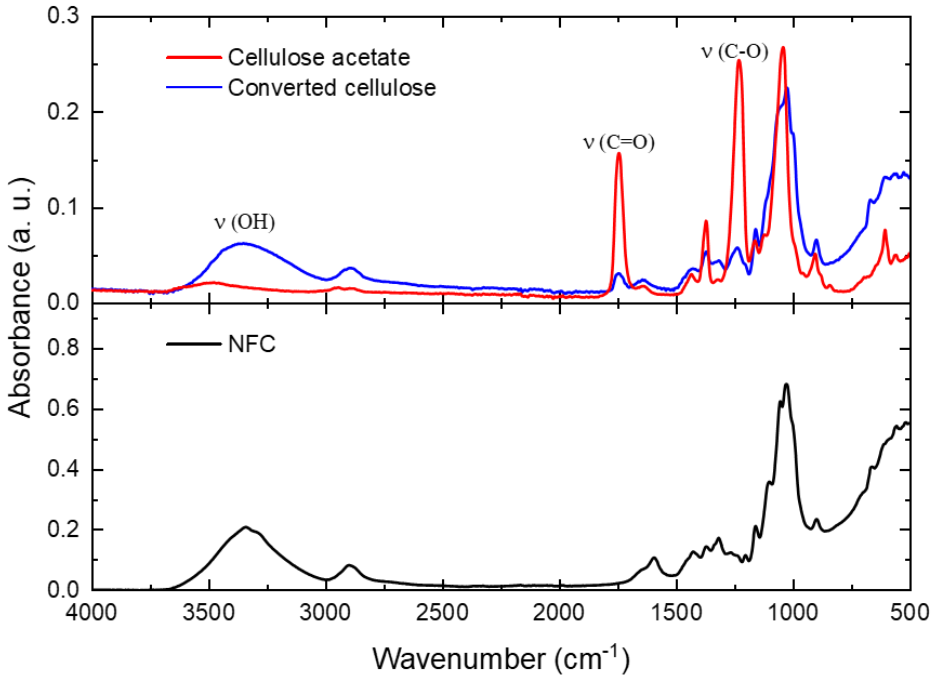

Figure S1. (top) FTIR spectra of cellulose acetate (red) and converted cellulose (blue). The significant decrease of the C=O and C-O mode peaks, and emergence of OH peak of the FTIR spectrum of converted cellulose indicate successful conversion of cellulose acetate to cellulose. (bottom) FTIR spectrum of a pure NFC sample (black) for comparison.

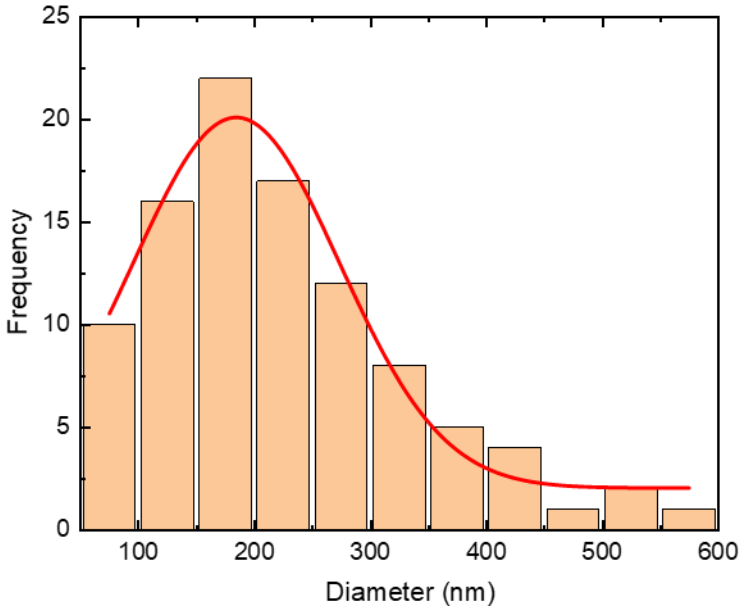

Figure S2. Cellulose fiber size distribution measured for an electrospun cellulose sample together with the Gaussian fit (red line) of the distribution.

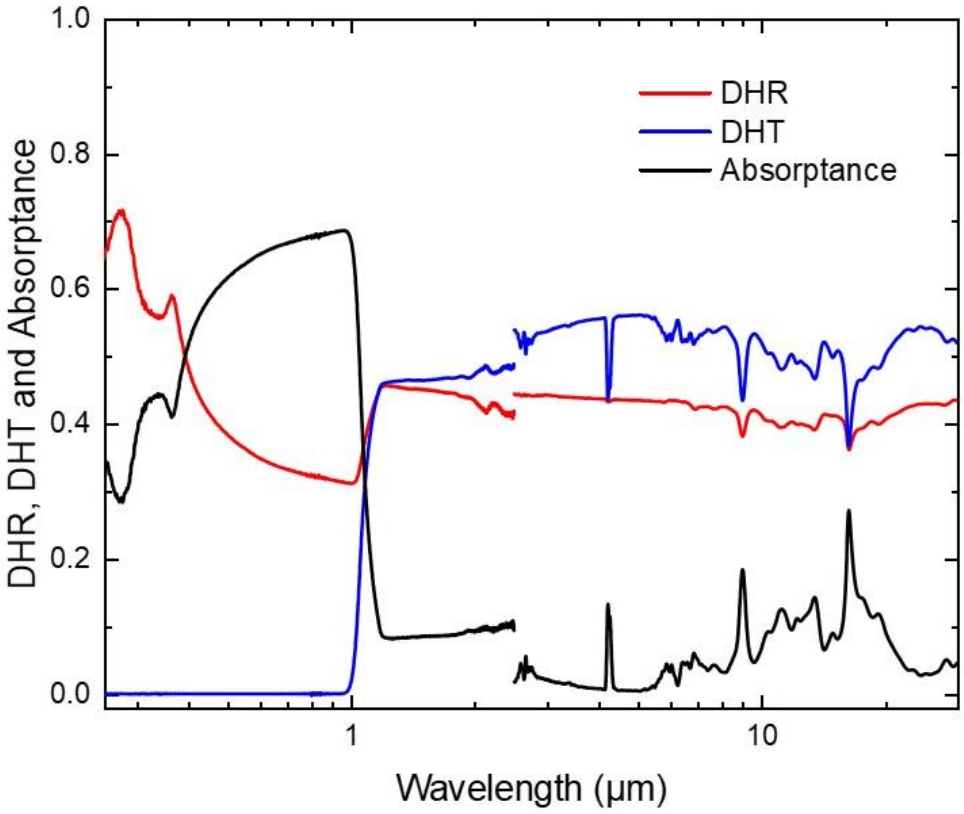

Figure S3. Optical properties of the same type of silicon wafer as used as reference and substrate. Total absorption (black line) was calculated using measured directional hemispherical reflectance (DHR) and directional hemispherical transmittance (DHT) given by red and blue lines, respectively. The DHR and DHT spectra for UV-Vis-NIR and MIR regions were obtained using two different spectrometers.

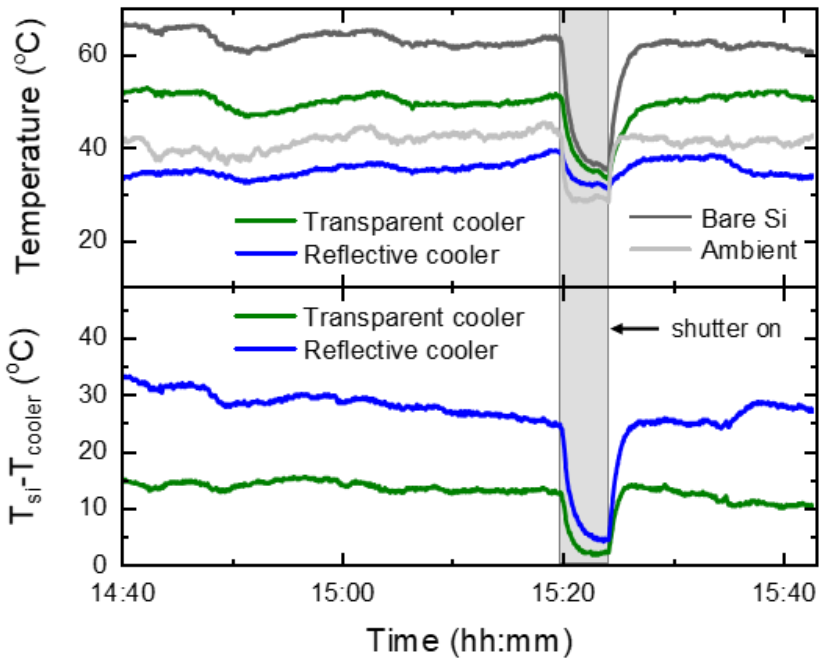

Figure S4. Temperature measurement of reflective and transparent coolers (different but similar to the samples used in Fig. 4) and bare silicon wafer during daytime in Norrköping, Sweden on another sunny day with clear sky (May 22, 2020). For this measurement, the ambient temperature was measured with a partially shaded thermocouple. The grey-shaded region corresponds to a period when the setup was shaded.

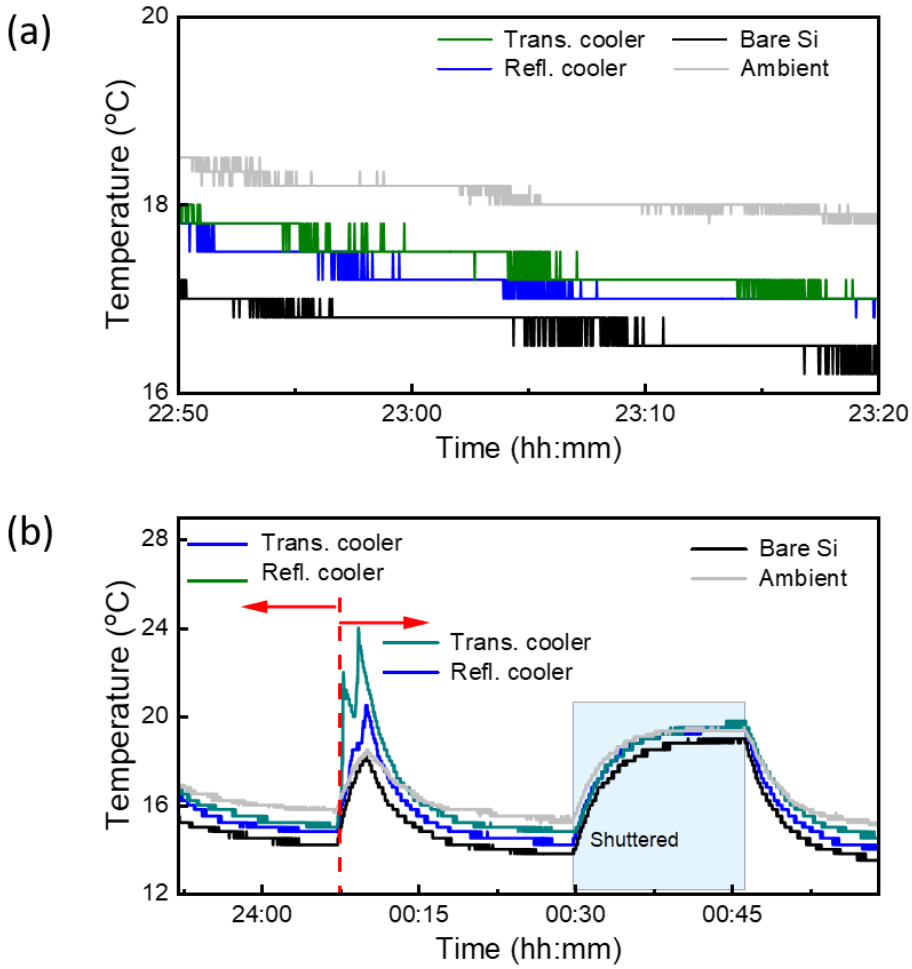

Figure S5. Temperature measurements during nighttime for the same reflective and transparent coolers as used for Fig. 4, with the ambient temperature presented as the average of two shaded thermocouples in the same box. Results during a short time period is presented in (a), while (b) shows results for a longer time period. The red dashed line in (b) indicate a time at which we switched places in the box between the reflective and transparent coolers (after which some re-equilibration takes place). Both coolers consistently provided subambient cooling when exposed to the sky, while their temperatures overlapped with the ambient temperature if when the measurement box was shuttered (blue-shaded period). The bare silicon also showed subambient temperatures, although we also note that its measured temperature was lower also then the ambient also during the shuttered period, by contrast to the results for the two coolers. We also note that the temperature in the whole box was (≈4 °C) higher during the shuttered/shaded time period, indicating that the samples may cool larger parts of the box and effectively lower also the temperature measured by the ambient thermocouples and thereby underestimate the cooling performance. For the same reason, the temperature of the bare silicon sample, positioned in the middle between the two coolers, may be partially cooled by the two surrounding coolers.

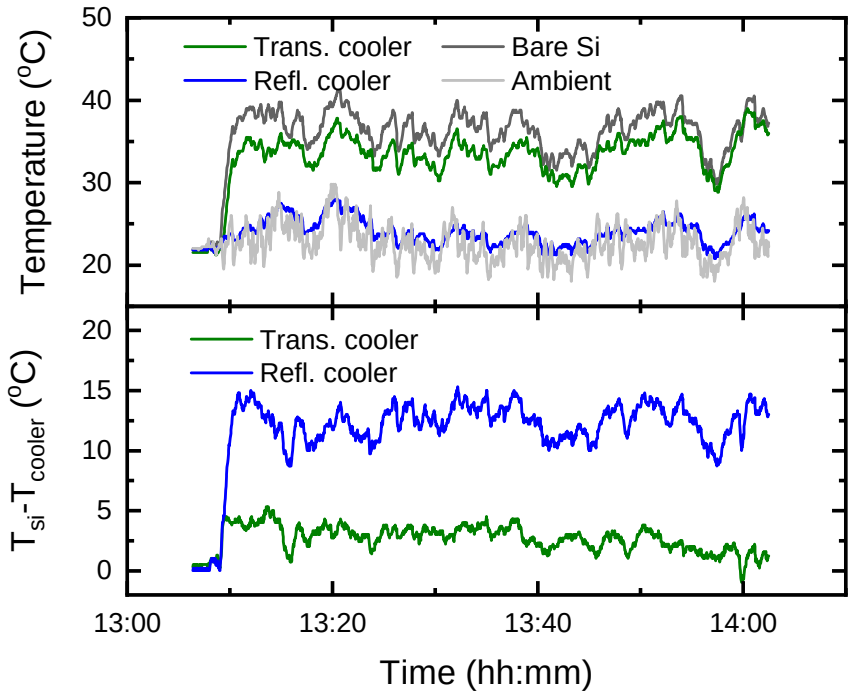

Figure S6. Temperature measurement of reflective and transparent coolers and a bare silicon wafer during daytime on a sunny day with clear sky, without the wind barrier. Temperature reduction of the two types of coolers relative to the temperature of bare silicon wafer is given in the bottom panel. For this measurement, the ambient temperature was measured with a partially shaded thermocouple. The setup was taken outside at around 13.10.

Cooling power density calculations

The net cooling power density, P_{net} is given by (Zaman et al. 2019).

$$P_{\text{net}} = P_{\text{rad}} - P_{\text{atm}} - P_{\text{nonrad}} - P_{\text{solar}} \quad \text{Eq 1}$$

where P_{rad} is the thermal radiation power per area of the cooler, P_{atm} is the power per area absorbed by the cooler due to incident radiation from the atmosphere, P_{nonrad} accounts for power lost or gained due to conduction and convection, and P_{solar} corresponds to incident absorbed power per area from solar irradiation.

P_{rad} is given by:

$$P_{\text{rad}} = \int_{\Omega} \cos(\theta) \int_0^{\infty} I_{BB}(\lambda, T)\varepsilon(\lambda, \theta)\mathrm{d}\lambda \, \mathrm{d}\Omega \quad \text{Eq 2}$$

where $I_{BB}(\lambda, T)$ is the thermal emission spectrum of a perfect black body at temperature T, Ω is the solid angle of a hemisphere and $\varepsilon(\lambda, \theta)$ is the emissivity (absorption) of the cooler, which we assume to be angle-independent and equal to the absorption of the cooling coating in our calculations. P_{rad} can then be calculated via the simplified equation:

$$P_{\text{rad}}(T) = \pi \int_0^{\infty} I_{BB}(\lambda, T)\varepsilon(\lambda)\mathrm{d}\lambda \quad \text{Eq 3}$$

where we used $\int_{\Omega} \cos(\theta)\, \mathrm{d}\Omega = 2\pi \int_{\theta=0}^{\pi/2} \sin(\theta)\cos(\theta)\, \mathrm{d}\theta = \pi$ for integration over the hemisphere.

Similarly, P_{atm} can be obtained by

$$P_{\text{atm}}(T_{\text{amb}}) = \int_{\Omega} \cos(\theta) \int_0^{\infty} I_{BB}(\lambda, T_{\text{amb}})\varepsilon(\lambda, \theta)\varepsilon_{\text{atm}}(\lambda, \theta)\mathrm{d}\lambda \, \mathrm{d}\Omega \quad \text{Eq 4}$$

where T_{amb} is the ambient temperature and $\varepsilon_{\text{atm}}(\lambda, \theta)$ is the emissivity of the atmosphere, given by:

$$\varepsilon_{\text{atm}}(\lambda, \theta) = 1 - t_{\text{atm}}(\lambda)^{1/\cos(\theta)} \quad \text{Eq. 5}$$

where $t_{\text{atm}}(\lambda)$ is the atmospheric transmittance at zenith ($\theta = 0$). We then get:

$$P_{\text{atm}}(T_{\text{amb}}) = 2\pi \int_0^{\pi/2} \sin(\theta)\cos(\theta) \int_0^{\infty} I_{BB}(\lambda, T_{\text{amb}})\varepsilon(\lambda, \theta)\varepsilon_{\text{atm}}(\lambda, \theta)\mathrm{d}\lambda \, \mathrm{d}\theta. \quad \text{Eq. 6}$$

In our calculations, we calculated P_{rad} and P_{atm} using the same wavelength range (7μm - 13.9μm) and using the atmospheric transmittance data from Atmospheric Transmission, Gemini Observatory, 2005 for the latter.

P_{nonrad} can be estimated by:

$$P_{\text{nonrad}} = h_c(T_{\text{amb}} - T) \quad \text{Eq. 7}$$

where h_c is the nonradiative heat transfer coefficient, which we set to 6.9 W/(m^{2}K) or 20 W/(m^{2}K) in our calculations.

Finally, P_{solar} is given by:

$$P_{\text{solar}} = \int_0^{\infty} I_{\text{solar}}(\lambda)\alpha(\lambda)\mathrm{d}\lambda \quad \text{Eq. 8}$$

where $\alpha(\lambda)$ is the absorptance of the whole device and $I_{\text{solar}}(\lambda)$ is the effective solar irradiance on the cooler, which we estimate as the AM1.5 solar spectrum reduced to 0.8 sun based on measurements using a solar cell reference meter (Newport, model number 91150V) positioned next to the measurement system

and with same angle to the sun as the coolers. P_{solar} was calculated over the wavelength range 280nm to 13.9μm. We accounted for solar absorption not only by the cellulose cooling material but also by the underlying silicon substrate using:

$$\alpha(\lambda) = A_{\text{coating}}(\lambda) + T_{\text{coating}}(\lambda) \cdot A_{\text{Si}}(\lambda) + T_{\text{coating}}(\lambda) \cdot R_{\text{Si}}(\lambda) \cdot A_{\text{coating}}(\lambda) \quad \text{Eq. 9}$$

where $A_{\text{coating/Si}}$, $T_{\text{coating/Si}}$, and $R_{\text{coating/Si}}$ correspond to measured absorptance, transmittance and reflectance, respectively, for the coatings or the underlying silicon substrate.

Figure S7 shows the calculated results for the reflective (red/orange) and transparent (blue) coolers on silicon, using measured optical properties of the same coolers as used for the measurements presented in Fig. 4 in the main manuscript. We performed the calculations at two different ambient temperatures and for two different nonradiative heat transfer coefficients. The results are presented as P_{net} as a function of $T - T_{\text{amb}}$ (where T is the temperature of the cooler). For all calculated conditions, the reflective cooler provides positive net cooling power at $T - T_{\text{amb}} = 0$ °C while the transparent cooler shows negative values.

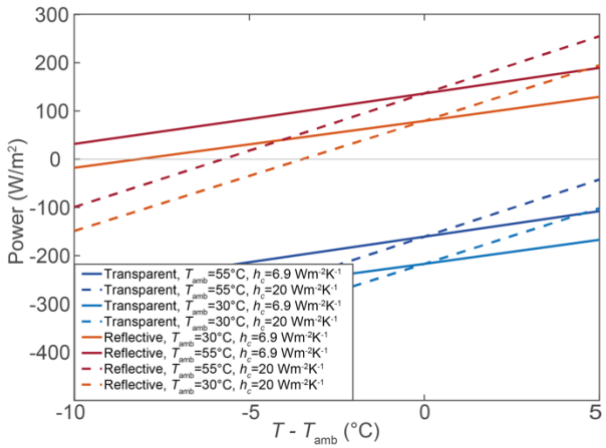

Figure S7. Calculated net cooling power density for the reflective (red) and transparent (blue) coolers on silicon at different $T - T_{\text{amb}}$.

References

Zaman. M. Asif (2019) Photonic radiative cooler optimization using Taguchi's method. International Journal of thermal science 144:21-26.

Atmospheric Transmission Data, Gemini Observatory, (2005) http://www.gemini.edu/sciops/instruments/mid-ir-resources/spectroscopic-calibrations/atmosphericstransmission-data.